Synthesis, Single Crystal, and Physical Properties of Asymmetrical Thiophene/Selenophene-Fused Twistacenes

ARTICLE *in* CHEMISTRY - AN ASIAN JOURNAL · AUGUST 2015

Impact Factor: 4.59 · DOI: 10.1002/asia.201500733 · Source: PubMed

6 AUTHORS, INCLUDING:

Xingxing Shen

Chinese Academy of Sciences

11 PUBLICATIONS **6** CITATIONS

SEE PROFILE

Yuanping Yi

Chinese Academy of Sciences

82 PUBLICATIONS **1,558** CITATIONS

SEE PROFILE

ACES

DOI: 10.1002/asia.201500733

CHEMISTRY
AN ASIAN JOURNAL
Full Paper

Fluorescence

Synthesis, Single Crystal, and Physical Properties of Asymmetrical Thiophene/Selenophene-Fused Twistacenes

Bo Lv,[a] Xingxing Shen,[b] Jinchong Xiao,*[a] Jingdan Duan,[a] Xuefei Wang,[c] and Yuanping Yi*[b]

Abstract: Two asymmetrical twistacenes, **PyPT** and **PyPS**, have been synthesized and characterized. Single crystal X-ray analyses show that both of them have twisted structures with a torsion angle of 26.65° for **PyPT** and 26.59° for **PyPS** measured between plane C5-C23-C25 and plane C13-C15-C26. The thiophene/selenophene-fused acenes emit blue fluorescence with quantum yields of 0.39 for **PyPT** and 0.04 for **PyPS** in organic solvents, whereas the all-carbon molecule **HBP** emits green fluorescence. Meanwhile, **PyPT** and **PyPS** show a similar reversible oxide procedure with the onset potentials of 0.73 and 0.72 V, respectively. In addition, **PyPT** and **PyPS** can self-assemble to form nanoparticles in a mixture of THF/H_2O through re-precipitation method.

Introduction

In the past decades, the preparation of large acenes, usually consisting of linearly-fused benzene rings, has been a focus of scientific research because these derivatives can be used as candidates in next-generation flexible electronics, such as light-emitting diodes, field-effect transistors, and photovoltaic cells.[1–5] For example, rubrene was doped into aluminum 8-hydroxyquinolinate (AlQ_3) or *N*,*N*′-bis(3-methylphenyl)-*N*,*N*′-bis(phenyl)benzidine (TPD) to fabricate organic electroluminescent devices that emitted strong luminance.[6] Additionally, the transistor based on its single crystals presented the mobility as high as 40 cm^2V^{-1}.[7] Recently, Zimmerman and co-workers predicted that singlet fission could occur in pentacene, which was beneficial for the rational design of photovoltaic materials.[8] Subsequently, Swager and Parkhurst synthesized a new type of ladder-type phenylene-containing oligoacenes that may participate in the singlet fission process.[9] Thus, the systematic study of the design, synthesis, and functionalization of acenes remains a hot topic.

The rarity and non-existence of large linear acenes resulting from their poor solubility in most organic solvents and high reactivity, such as easy oxidation and photodimerization, have encouraged researchers to attempt multi-step synthesis approaches. To circumvent these detracting factors, triisopropylsilylethynyl (TIPS), phenyl, alkylthio or arylthio substituents were grafted onto the main acene framework, causing the electrons to delocalize through the entire molecule and thus suppressing their reactivity under ambient conditions.[10] When pyrene units are linked to the terminal position of these acenes, symmetric and asymmetric acenes can be obtained. More interestingly, the resulting molecules can twist as a result of the steric hindrance, which effectively enhances their stability and processability without sacrificing other physical properties. The research groups of Wudl and Zhang reported a series of twistacenes and tested their electroluminescence properties.[11] In addition, some pyrene-fused twistacenes and π-conjugated dendrimers were also synthesized in our laboratory.[12] Another strategy is to incorporate the parent skeletons with heteroatoms,[13] which can affect the crystal packing arrangement and tune the optoelectronic properties. For example, the interplanar distance in chrysene single crystals is 5.07 Å, whereas its analogue, 6,6,13,13-tetrafluoro-6,13-dihydropyrido[1,2-c]pyrido-[1′,2′:3,4][1,3,2] oxazaborinino[6,5-e][1,3,2]oxazaborinine-7,14-diium-6,13-diuide, has an average intermolecular distance of 3.30 Å.[14] Furthermore, aryl-substituted tetrathiaheptacenes possess chair conformations in contrast to planar heptacene.[15] Clearly, substitution of the C–H moiety in acenes with heteroatoms can produce electron- and hole-transporting materials. These intriguing merits inspire us to prepare heterotwistacenes for extending functional applications.

[a] *B. Lv, Prof. J. Xiao, J. Duan*
College of Chemistry and Environmental Science
Key Laboratory of Chemical Biology of Hebei Province
Hebei University
Baoding 071002 (P. R. China)
E-mail: jcxiaoicas@163.com

[b] *X. Shen, Prof. Y. Yi*
Key Laboratory of Organic Solids
Beijing National Laboratory for Molecular Science (BNLMS)
Institute of Chemistry
Chinese Academy of Sciences
Beijing, 100190 (P. R. China)
E-mail: ypyi@iccas.ac.cn

[c] *Prof. X. Wang*
School of Chemistry and Chemical Engineering of University of Chinese Academy of Sciences
Beijing 100049 (P. R. China)

Supporting information for this article is available on the WWW under http://dx.doi.org/10.1002/asia.201500733.

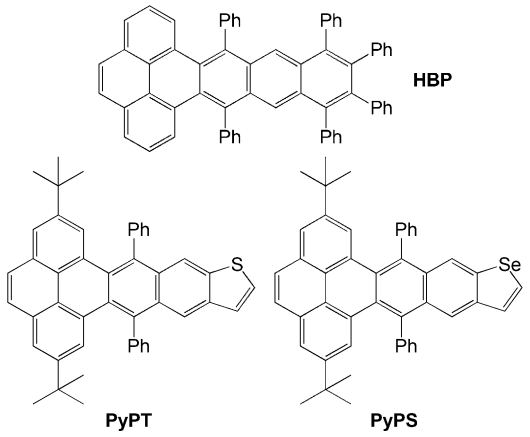

Scheme 1. Chemical structures of **HBP**, **PyPT** and **PyPS**.

In this study, two asymmetric heteroacenes (**PyPT** and **PyPS**) were successfully synthesized and fully characterized (Scheme 1). Clearly, substitution of the terminal phenyl group in **HBP**[11d] with the thiophene and selenophene units affords the heteroacenes **PyPT** and **PyPS**, respectively. The X-ray analyses showed fused acenes displaying a twisted topological configuration. Their corresponding optical, redox and thermal properties were further measured. The effect of chalcogenation on the physical properties was also studied in a comparative manner.

Results and Discussion

The synthetic routes for the twistacenes **PyPT** and **PyPS** are outlined in Scheme 2. The black precursor, **1**, which is reported elsewhere, was treated with 2-amino-4,5-dibromobenzoic acid (**2**) to yield the desired green solid, **3** (51%), by treatment with isoamyl nitrile in anhydrous 1,2-dichloroethane (DCE) at refluxing temperature.[12] A subsequent selective reaction between **3** and trimethylsilyl acetylene (**4**) was completed through a Sonogashira coupling catalyzed by $[PdCl_2(PPh_3)_2]$, PPh_3, and CuI in a triethylamine solution to afford **5** in 27% yield. Subsequently, the target molecules, **6** (**PyPT**, 40%) and **7** (**PyPS**, 22%), were generated through cyclization of **5** with $Na_2S{\cdot}9H_2O$ or Se/$NaBH_4$, respectively, in 1-methyl-2-pyrrolidone (NMP) according to the reported method.[16] The introduction of *tert*-butyl groups onto these twistacenes can effectively enhance their solubility in common organic solvents such as dichloromethane, chloroform, 1,2-dichlorobenzene (ODCB), and toluene; this is beneficial for characterization using ^1H NMR, ^{13}C NMR, MALDI-TOF and HRMS spectrometry (see the Supporting Information). In addition, the thermal properties of **PyPT** and **PyPS** were examined through thermal gravimetric analysis (TGA) under a nitrogen atmosphere at a heating rate of 10 °C min^{-1} (see Figure S1 in the Supporting Information). The onset curves of 5% weight loss begin at 356 °C for **PyPT** and 380 °C for **PyPS**. Figure S2 (see the Supporting Information) presents the differential scanning calorimetry (DSC) traces of **PyPT** and **PyPS**. No phase transition was observed between 50–300 °C. Meanwhile, the DSC curves increased slightly above approximately 200 °C, which may be a result of the softening of the molecules. By taking the TGA and DSC results into consideration, we believe that the resulting compounds have high thermal stability. Note that **PyPT** and **PyPS** are very stable in the solid state under ambient conditions and can be stored indefinitely.

The single crystals of **PyPT** and **PyPS** were prepared by evaporation of a CH_2Cl_2/CH_3OH mixture solution. The molecular structures and packing modes are shown in Figure 1. Crystal data and atomic coordinates are given in Tables S1–S4 (see the Supporting Information). They both adopt a monoclinic unit cell. The space groups are *P*21/*n* for **PyPT** and *P*21/*c* for **PyPS**. The unit cell dimensions are observed as follows: $a=$ 15.7237 Å, $b=10.1948$ Å, $c=$ 21.2943 Å, $\alpha=90°$, $\beta=100.685°$, $\gamma=90°$ for **PyPT** (CCDC: 1034509) and $a=15.8185$ Å, $b=$ 10.2356 Å, $c=24.115$ Å, $\alpha=90°$, $\beta=118.525°$, $\gamma=90°$ for **PyPS** (CCDC: 1063524).[16b] Both **PyPT** and **PyPS** have the twisted structures with the torsion angles of 26.65° and 26.59° measured between plane C5-C23-C25 and plane C13-C15-C26, respectively. These angles

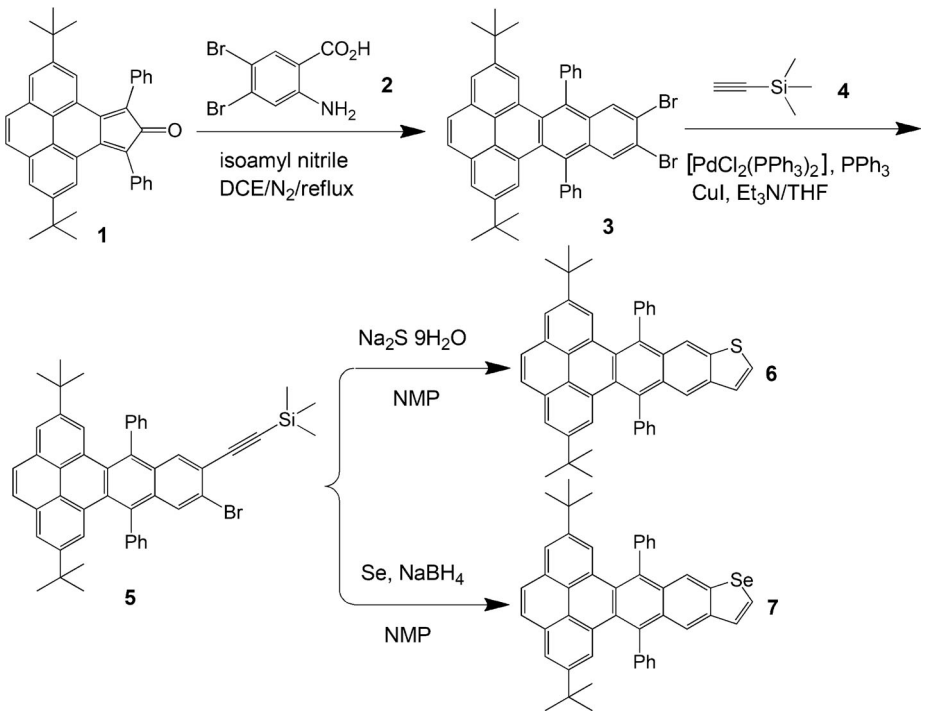

Scheme 2. Synthetic routes to **6** (**PyPT**) and **7** (**PyPS**).

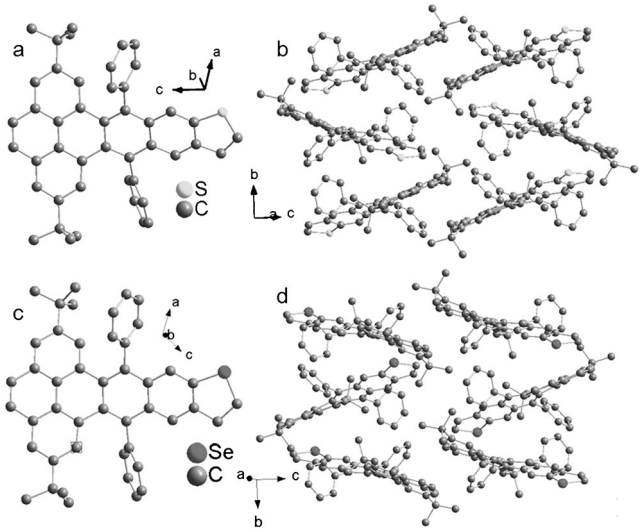

Figure 1. The intramolecular geometries and intermolecular packing modes in the **PyPT** (a, b) and **PyPS** (c, d) single crystals obtained by X-ray diffraction.

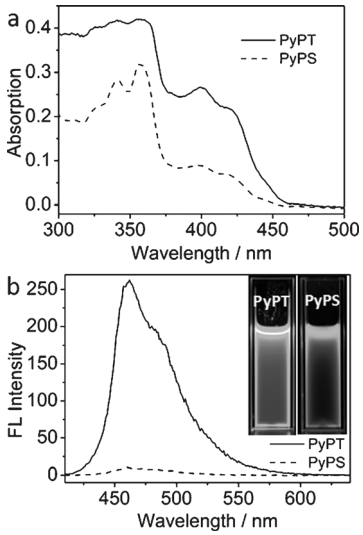

Figure 2. (a) UV-Vis absorption spectra and (b) emission spectra of **PyPT** and **PyPS** in dichloromethane at an excitation wavelength of 400 nm. Inset shows the fluorescence images excited at 365 nm.

are slightly larger than that of **HBP** (23.0°), indicating that the terminal thiophene/selenophen moieties have a little effect on the twisted topological configurations. As shown in the packing modes, each molecule of **PyPT** or **PyPS** slides on its neighboring one, thus largely avoiding the cofacial π–π stacking interaction. Figure S3 (see the Supporting Information) shows the optimized structures for the ground states of **PyPT** and **PyPS** based on density functional theory (DFT) calculations. Their backbones take a twisted configuration, and the torsion angles between pyrene unit and naphtha[2,3-b]thiophene/naphtha[2,3-b]selenophene groups are approximately 41° for both **PyPT** and **PyPS**, which are somewhat larger than those obtained from the experimental crystal structures. This can be attributed to the intermolecular interactions in single crystals, and a similar phenomenon was observed in oligothiophenes.[17]

The optical properties of **PyPT** and **PyPS** in diluted dichloromethane solutions at room temperature are shown in Figure 2 and Table 1. **PyPT** and **PyPS** displayed similar absorption profiles with five characteristic peaks at 324 nm, 340 nm, 356 nm, 400 nm, and 420 nm. Given their resemblance in molecular structure, the thiophene- and selenophene-linked molecules **PyPT** and **PyPS** have obvious hypochromic shifts in the lowest energy absorption bands compared to **HBP**, suggesting shorter π-conjugation. The optical band gaps of **PyPT** and **PyPS** can be calculated from the onset of the UV-Vis absorption spectra and are 2.77 and 2.78 eV, respectively; this is in good agreement with the first singlet excitation energy obtained by time-dependent DFT (TDDFT) calculations (see Table S5 in the Supporting Information). The emission spectra of **PyPT** and **PyPS** show blue–green fluorescence and a maximum band at 460 nm with a shoulder peak at 490 nm. In comparison to **HBP**, the centers of the emission bands are also blue-shifted by approximately 31 nm. The small Stokes shift between the absorption and fluorescence peaks of compounds **PyPT** and **PyPS** might be attributed to their rigid molecular structures. In addition, the fluorescence quantum yields (Φ_F) in dichloromethane are 0.39 for **PyPT** and 0.04 for **PyPS**, as determined by 9,10-diphenylanthracene ($\Phi_F = 0.95$ in ethanol)[12] as the reference standard. TDDFT calculations show that **PyPT** and **PyPS** display very similar energy alignments between the singlet and triplet states and the lowest singlet excited state (S_1) is lying close to the triplet states (see Table S6 in the Supporting Information). Thus, the lower quantum yield in **PyPS** can be assigned to faster intersystem crossing from S_1 to the triplet states due to the stronger spin-orbit coupling arising from the heavy atom effect.

Table 1. Photophysical and electrochemical properties of **HBP**, **PyPT,** and **PyPS**.

	HBP[11d]	**PyPT**	**PyPS**
Abs[a] [nm]	415, 446, 474	356, 400, 420	356, 400, 420
PL[a] [nm]	491, 521	460, 490	460, 490
Φ_f	0.69	0.39	0.04
$E_{1/2}^{ox}$ [V]	0.74	0.73	0.72
HOMO [eV]	−5.14	−5.13	−5.12
HOMO[b] [eV]		−4.99	−4.97
Band gap[c] [eV]	2.64	2.77	2.78
Band gap[b] [eV]		3.30	3.29

[a] in CH_2Cl_2. [b] Obtained from DFT calculation. [c] Derived from the onset of the UV-Vis data.

To further assess the electronic structures and assign the energy levels of the frontier orbitals, cyclic voltammetry of **PyPT** and **PyPS** was performed at room temperature. The results are shown in Figure 3 and Table 1. **PyPT** and **PyPS** exhibit their first reversible oxidation processes at half-wave potentials of approximately 0.73 V and 0.72 V, respectively. These values are very close to their counterpart, **HBP** ($E_{1/2}^{ox} = +0.74$ V) and are attributed to the oxidation of the π-conjugated core scaffold. Based on the first reversible oxidation potentials, the

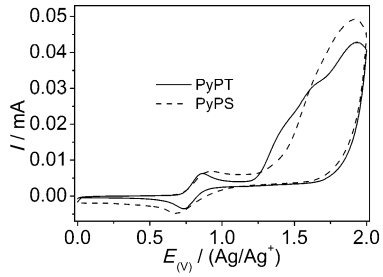

Figure 3. Cyclic voltammograms of **PyPT** and **PyPS** in anhydrous dichloromethane.

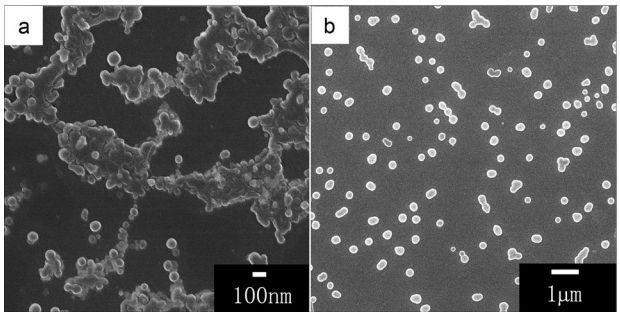

Figure 5. SEM images of **PyPT** (a) and **PyPS** (b) using CTAB as the surfactant.

highest occupied molecular orbital (HOMO) energy levels were determined to be −5.13 eV and −5.12 eV according to the empirical equation,[18] which are lower than the DFT calculated results by 0.14 eV presumably due to the solvent polarization effects.[19] As shown in Figure 4, the frontier orbital profiles for

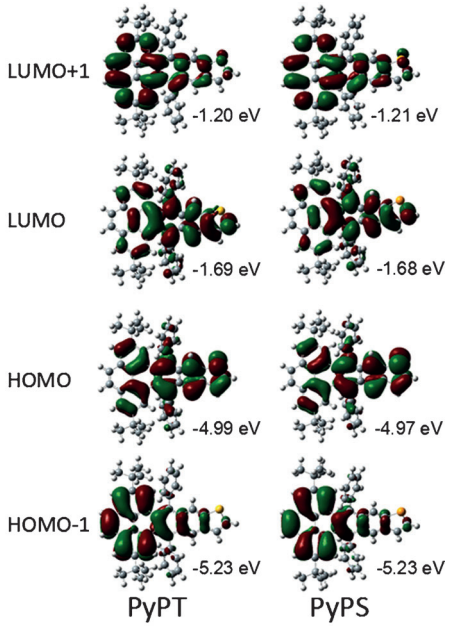

Figure 4. The frontier molecular orbital profiles of **PyPT** and **PyPS**.

PyPT and **PyPS** are almost the same. The HOMO and LUMO are distributed over the whole molecular backbone except the four lateral carbon atoms in the pyrene unit. The band gap between the HOMO and LUMO is estimated to be approximately 3.3 eV by DFT calculations.

The self-assembly behavior of compounds **PyPT** and **PyPS** was studied using a re-precipitation method with hexadecyl trimethyl ammonium bromide (CTAB) as a soft template (Figure 5).[20] The obtained molecules, **PyPT** or **PyPS**, dissolved in THF were added to a solution of CTAB in water under strong stirring. After maintaining the solution at room temperature overnight, the aggregated structures were observed using scanning electron microscopy (SEM). The SEM images display that **PyPT** and **PyPS** (the volume of THF to CTAB was 1:5) can form a large area of nanoparticles with diameters of 30–150 nm and 190–400 nm, respectively. When the volume of THF/CTAB is increased to 1:11, similar nanoparticles were observed (see Figure S4 in the Supporting Information), indicating that the solvent volume ratio has a negligible effect on the aggregation morphology for **PyPT** and **PyPS**.

Conclusions

In summary, we have presented the synthesis of two novel asymmetrical twistacenes, **PyPT** and **PyPS**, containing terminal thiophene or selenophene units, respectively. Both compounds emit blue fluorescence in dichloromethane, rather than the green light emitted by **HBP**, because of the decreased π-conjugation. Moreover, the chalcogenation with sulfur and selenium have some effect on the electrochemical and thermal properties to a certain extent. Ordered nanoparticles have been obtained through a re-precipitation method by tuning the ratio of THF to H_2O. We believe that such molecular design would be beneficial for enriching the chemistry of graphene fragments. Further functionalization and exploration of their potential application in organic electronics will be underway in the near future.

Experimental Section

Synthesis of compound 3

Isoamyl nitrite (1 mL) and 2-amino-4,5-dibromobenzoic acid (**2**, 294 mg, 1.0 mmol), dispersed in degassed 1,2-dichloroethane (DCE, 5 mL), were alternatively added slowly into a solution of the black solid **1** (518 mg, 1.0 mmol) and heated in refluxing DCE (15 mL) under a nitrogen atmosphere. After 12 h, the mixed solution was cooled to room temperature. Brine (100 mL) was then added to the solution and the resulting mixture was extracted with dichloromethane (40 mL×3). The organic phase was then dried over anhydrous sodium sulfate. The organic solvent was evaporated and the residue was purified using column chromatography on silica gel to afford **3** from petroleum ether as a light yellow solid (368 mg, 51%). M.p.: 315–318 °C; ^{1}H NMR (600 MHz, $CDCl_3$, 298 K): δ = 8.10 (s, 2H), 8.09 (d, J = 1.8 Hz, 2H), 7.86 (d, J = 1.8 Hz, 2H), 7.84 (s, 2H), 7.59–7.54 (m, 8H), 7.50 (t, J = 7.2 Hz, 2H), 1.11 ppm (s, 18H); ^{13}C NMR (150 MHz, $CDCl_3$, 298 K): δ = 147.4, 141.6, 135.1, 132.2, 131.9, 131.2, 131.1, 130.4, 129.6, 129.0, 128.0, 127.7, 127.0, 123.9, 122.8, 122.0, 34.8, 31.5 ppm; MS (MALDI-TOF): calcd for $C_{44}H_{36}Br_2$: $[M]^+$ 722.1, found: $[M]^{2+}$ 724.0; HRMS: $C_{44}H_{36}Br_2$, calcd m/z = 722.1184; found m/z = 722.1178.

Synthesis of compound 5

A mixture of compound **3** (200 mg, 0.276 mmol), $[PdCl_2(PPh_3)_2]$ (11 mg, 0.015 mmol), CuI (3 mg, 0.015 mmol), PPh_3 (4 mg, 0.015 mmol), trimethylsilylacetylene (**4**, 27 mg, 0.276 mmol), and triethylamine (15 mL) was stirred at 90 °C under a nitrogen atmosphere. After 24 h, the solution was cooled and then extracted with dichloromethane (40 mL×3). The organic phase was washed with brine (50 mL×3), dried over sodium sulfate, and concentrated under reduced pressure. The residue was purified using column chromatography on silica gel (petroleum ether) to afford **5** (yellow solid, 55 mg, 27%). M.p.: 206–207 °C; ^{1}H NMR (600 MHz, $CDCl_3$, 298 K): δ = 8.10 (d, J = 1.2 Hz, 1H), 8.07 (d, J = 1.2 Hz, 1H), 8.05 (s, 1H), 8.01 (s, 1H), 7.85 (s, 2H), 7.84 (s, 2H), 7.59–7.53 (m, 8H), 7.51–7.47 (m, 2H), 1.11 (s, 18H), 0.29 ppm (s, 9H); ^{13}C NMR (150 MHz, $CDCl_3$, 298 K): δ = 147.5, 141.9, 141.8, 136.0, 135.1, 132.5, 132.5, 132.4, 131.8, 130.8, 130.5, 129.9, 129.7, 129.6, 129.3, 129.2, 128.02, 128.0, 127.8, 127.7, 127.1, 127.0, 124.1, 124.0, 122.9, 122.8, 122.3, 122.0, 104.1, 99.8, 34.9, 31.5, 31.48 ppm; MS (MALDI-TOF): calcd for $C_{49}H_{45}BrSi$: $[M]^+$ 740.25, found: $[M]^{2+}$ 742.5; HRMS: $C_{49}H_{45}BrSi$, calcd m/z = 740.2474; found m/z = 740.2468.

Synthesis of compound 6

A mixture of compound **5** (150 mg, 0.2 mmol), $Na_2S{\cdot}9H_2O$ (96 mg, 0.4 mmol), and NMP (15 mL) was stirred at 195 °C under a nitrogen atmosphere overnight. After cooling to room temperature, brine (80 mL) was added and then the mixture was extracted with dichloromethane (40 mL×3). The organic phase was dried over sodium sulfate and concentrated. The obtained residue was further purified using column chromatography on silica gel with petroleum ether as the eluent to afford the target molecule **6** (yellow solid, 50 mg, 40%). M.p.: 338–340 °C; ^{1}H NMR (600 MHz, $CDCl_3$, 298 K): δ = 8.36 (s, 1H), 8.30 (s, 1H), 8.12 (d, J^1 = 4.2 Hz, J^2 = 1.2 Hz, 2H), 7.83 (s, 2H), 7.81 (d, J = 1.8 Hz, 2H), 7.66–7.64 (m, 4H), 7.60 (t, J = 7.8 Hz, 4H), 7.52–7.47 (m, 3H), 7.35 (d, J = 6.0 Hz, 1H), 1.12 ppm (s, 18H); ^{13}C NMR (150 MHz, $CDCl_3$, 298 K): δ = 147.3, 142.9, 142.87, 138.7, 138.3, 132.6, 130.3, 130.2, 129.8, 129.5, 129.4, 129.2, 128.8, 128.5, 127.8, 127.7, 127.6, 127.56, 126.9, 124.0, 123.97, 123.9, 122.3, 122.2, 121.0, 119.7, 34.8, 31.4 ppm; MS (MALDI-TOF): calcd for $C_{46}H_{38}S$: $[M]^+$ 622.3, found: $[M]^+$ 622.4; HRMS: $C_{46}H_{38}S$, calcd m/z = 622.2694; found m/z = 622.2689.

Synthesis of compound 7

Sodium borohydride (30 mg, 0.8 mmol) was added to a solution of selenium (63 mg, 0.8 mmol) in ethanol (5 mL) at 0 °C under a nitrogen atmosphere. The solution was stirred for 40 min and then an NMP (12 mL) solution of compound **5** (150 mg, 0.2 mmol) was added. Ethanol was evaporated by distillation. The mixture was stirred overnight at 190 °C. After cooling to room temperature, water and ethyl acetate were added. The collected organic phase was then washed with brine (50 mL×3), the solution was dried over sodium sulfate, and the organic solvent was removed under reduced pressure. The formed residue was purified using column chromatography on silica gel (petroleum ether) to afford **7** (yellow solid, 30 mg, 22%). M.p.: 358–360 °C; ^{1}H NMR (600 MHz, $CDCl_3$, 298 K): δ = 8.37 (s, 1H), 8.28 (s, 1H), 8.12 (dd, J^1 = 4.2 Hz, J^2 = 1.8 Hz, 2H), 7.95 (d, J = 6.0 Hz, 1H), 7.83 (d, J = 7.8 Hz, 4H), 7.65 (d, J = 7.2 Hz, 4H), 7.60–7.58 (m, 4H), 7.56 (d, J = 6.0 Hz, 1H), 7.50 (t, J^1 = 7.8 Hz, J^2 = 7.2 Hz, 2H), 1.12 ppm (s, 18H); ^{13}C NMR (150 MHz, $CDCl_3$, 298 K): δ = 147.5, 143.0, 142.97, 141.3, 138.6, 136.4, 135.1, 132.8, 132.75, 130.5, 130.4, 130.3, 130.0, 129.9, 129.6, 129.5, 129.51, 129.1, 128.2, 127.91, 127.9, 127.8, 127.0, 124.13, 124.1, 123.1, 123.0, 122.4, 122.35, 34.9, 31.5 ppm; MS (MALDI-TOF): calcd for $C_{46}H_{38}Se$: $[M]^+$ 670.2, found: $[M]^+$ 670.4; HRMS: $C_{46}H_{38}Se$, calcd m/z = 670.2139; found m/z = 670.2138.

Density functional theory calculations

The ground state geometries for **PyPT** and **PyPS** were optimized by DFT at the B3LYP/6-31G** level. No imaginary frequencies were found for the optimized geometries through frequency analysis calculations. Based on the optimized geometries, the excitation energies for the lowest singlet and triplet excited states were calculated by TDDFT at the B3LYP/6-31G** level. All these calculations were carried out with the Gaussian 09 program.[21]

Acknowledgements

This work was supported by the National Natural Science Foundation of China (21102031, 21442010 and 91233107), the Natural Science Foundation of Hebei Province for Distinguished Young Scholar (Cultivation Project, B2015201183), the Natural Science Foundation of Hebei Province (B2014201007), the Strategic Priority Research Program of the Chinese Academy of Sciences (XDB12020200) and the Overseas Students Foundation of Hebei Province for Financial Support (C2012003048).

Keywords: heteroacenes · optical property · self-assembly · synthesis · twisted structures

[1] a) E. Clar, *Polycyclic Hydrocarbons*, Academic Press, London, **1964**; b) J. E. Anthony, *Chem. Rev.* **2006**, *106*, 5028; c) J. E. Anthony, *Angew. Chem. Int. Ed.* **2008**, *47*, 452; *Angew. Chem.* **2008**, *120*, 460; d) M. J. Bruzek, J. E. Anthony, *Org. Lett.* **2014**, *16*, 3608.

[2] a) M. Bendikov, F. Wudl, D. F. Perepichka, *Chem. Rev.* **2004**, *104*, 4891; b) T. V. Pho, J. D. Yuen, J. A. Kurzman, B. G. Smith, M. Miao, W. T. Walker, R. Seshadri, F. Wudl, *J. Am. Chem. Soc.* **2012**, *134*, 18185; c) A. Briseno, Q. Miao, M. M. Ling, C. Reese, H. Meng, Z. Bao, F. Wudl, *J. Am. Chem. Soc.* **2006**, *128*, 15576.

[3] a) A. A. Gorodetsky, M. Cox, N. J. Tremblay, I. Kymissis, C. Nuckolls, *Chem. Mater.* **2009**, *21*, 4090; b) Q. Miao, X. Chi, S. Xiao, R. Zeis, M. Lefenfeld, T. Siegrist, M. L. Steigerwald, C. Nuckolls, *J. Am. Chem. Soc.* **2006**, *128*, 1340.

[4] a) Q. Ye, C. Chi, *Chem. Mater.* **2014**, *26*, 4046; b) Q. Ye, J. Chang, K. Huang, G. Dai, J. Zhang, Z. Chen, J. Wu, C. Chi, *Org. Lett.* **2012**, *14*, 2786.

[5] a) M. Watanabe, Y. J. Chang, S. W. Liu, T. H. Chao, K. Goto, M. M. Islam, C. H. Yuan, Y. T. Tao, T. Shinmyozu, T. J. Chow, *Nat. Chem.* **2012**, *4*, 574; b) Y. Li, L. Xu, T. Liu, Y. Yu, H. Liu, Y. Li, D. Zhu, *Org. Lett.* **2011**, *13*, 5692; c) M. L. Tang, A. D. Reichardt, N. Miyaki, R. M. Stoltenberg, Z. Bao, *J. Am. Chem. Soc.* **2008**, *130*, 6064; d) C. L. Song, C. B. Ma, F. Yang, W. Zeng, H. Zhang, X. Gong, *Org. Lett.* **2011**, *13*, 2880.

[6] G. Mueller, *Semiconductors and Semimetals, Vol. 64*, Academic Press, **2000**.

[7] T. Hasegawa, J. Takeya, *Sci. Technol. Adv. Mater.* **2009**, *10*, 024314.

[8] P. M. Zimmerman, Z. Zhang, C. B. Musgrave, *Nat. Chem.* **2010**, *2*, 648.

[9] R. R. Parkhurst, T. M. Swager, *J. Am. Chem. Soc.* **2012**, *134*, 15351.

[10] a) I. Kaur, M. Jazdzyk, N. N. Stein, P. Prusevich, G. P. Miller, *J. Am. Chem. Soc.* **2010**, *132*, 1261; b) D. Chun, Y. Cheng, F. Wudl, *Angew. Chem. Int. Ed.* **2008**, *47*, 8380; *Angew. Chem.* **2008**, *120*, 8508; c) B. Purushothaman, M. Bruzek, S. R. Parkin, A. F. Miller, J. E. Anthony, *Angew. Chem. Int. Ed.* **2011**, *50*, 7013; *Angew. Chem.* **2011**, *123*, 7151; d) J. Wang, K. Liu, Y. Liu, C. Song, Z. Shi, J. Peng, H. Zhang, X. Cao, *Org. Lett.* **2009**, *11*, 2563.

[11] a) J. Xiao, H. M. Duong, Y. Liu, W. Shi, L. Ji, G. Li, S. Li, X. Liu, J. Ma, F. Wudl, Q. Zhang, *Angew. Chem. Int. Ed.* **2012**, *51*, 6094; *Angew. Chem.* **2012**, *124*, 6198; b) J. Xiao, C. D. Malliakas, Y. Liu, F. Zhou, G. Li, H. Su, M. G. Kanatzidis, F. Wudl, Q. Zhang, *Chem. Asian J.* **2012**, *7*, 672; c) J. Xiao, S. Liu, Y. Liu, L. Ji, X. Liu, H. Zhang, X. Sun, Q. Zhang, *Chem. Asian*

J. **2012**, *7*, 561; d) J. Xiao, Y. Divayana, Q. Zhang, H. M. Doung, H. Zhang, F. Boey, X. Sun, F. Wudl, *J. Mater. Chem.* **2010**, *20*, 8167; e) Q. Zhang, Y. Divayana, J. Xiao, Z. Wang, E. R. T. Tiekink, H. M. Doung, H. Zhang, F. Boey, X. Sun, F. Wudl, *Chem. Eur. J.* **2010**, *16*, 7422; f) J. Li, Q. Zhang, *Synlett* **2013**, *24*, 686; g) G. Li, H. M. Duong, Z. Zhang, J. Xiao, L. Liu, Y. Zhao, H. Zhang, F. Huo, S. Li, J. Ma, F. Wudl, Q. Zhang, *Chem. Commun.* **2012**, *48*, 5974; h) H. M. Duong, M. Bendikov, D. Steiger, Q. Zhang, G. Sonmez, J. Yamada, F. Wudl, *Org. Lett.* **2003**, *5*, 4433; i) Q. Xu, H. M. Duong, F. Wudl, Y. Yang, *Appl. Phys. Lett.* **2004**, *85*, 3357; j) J. Li, Y. Zhao, J. Lu, G. Li, J. Zhang, Y. Zhao, X. Sun, Q. Zhang, *J. Org. Chem.* **2015**, *80*, 109; k) J. Li, P. Li, J. Wu, J. Gao, W. Xiong, G. Zhang, Y. Zhao, Q. Zhang, *J. Org. Chem.* **2014**, *79*, 4438.

[12] a) Z. Liu, J. Xiao, Q. Fu, H. Feng, X. Zhang, T. Ren, S. Wang, D. Ma, X. Wang, H. Chen, *ACS Appl. Mater. Interfaces* **2013**, *5*, 11136; b) J. Xiao, Z. Liu, X. Zhang, W. Wu, T. Ren, B. Lv, L. Jiang, X. Wang, H. Chen, W. Su, J. Zhao, *Dyes Pigm.* **2015**, *112*, 176; c) X. Zhang, H. Song, J. Xiao, T. Ren, S. Wang, Z. Liu, X. Ba, Y. Wu, *Aust. J. Chem.* **2015**, *68*, 505.

[13] a) W. Jiang, Y. Li, Z. Wang, *Chem. Soc. Rev.* **2013**, *42*, 6113; b) X. Yin, Y. Li, Y. Zhu, Y. Kan, Y. Li, D. Zhu, *Org. Lett.* **2011**, *13*, 1520; c) G. Li, Y. Wu, J. Gao, C. Wang, J. Li, H. Zhang, Y. Zhao, Y. Zhao, Q. Zhang, *J. Am. Chem. Soc.* **2012**, *134*, 20298; d) P. Gu, F. Zhou, J. Gao, G. Li, C. Wang, Q. Xu, Q. Zhang, J. Lu, *J. Am. Chem. Soc.* **2013**, *135*, 14086; e) G. Li, Y. Wu, J. Gao, J. Li, Y. Zhao, Q. Zhang, *Chem. Asian J.* **2013**, *8*, 1574; f) J. Li, Q. Zhang, *ACS Appl. Mater. Interfaces* **2015**, DOI: 10.1021/acsami.5b00113; g) Y. Wu, Z. Yin, J. Xiao, Y. Liu, F. Wei, K. J. Tan, C. Kloc, L. Huang, Q. Yan, F. Hu, H. Zhang, Q. Zhang, *ACS Appl. Mater. Interfaces* **2012**, *4*, 1883; h) G. Li, K. Zheng, C. Wang, K. S. Leck, F. Hu, X. Sun, Q. Zhang, *ACS Appl. Mater. Interfaces* **2013**, *5*, 6458.

[14] H. Zhang, X. Hong, X. Ba, B. Yu, X. Wen, S. Wang, X. Wang, L. Liu, J. Xiao, *Asian J. Org. Chem.* **2014**, *3*, 1168.

[15] T. Ren, J. Xiao, W. Wang, W. Xu, S. Wang, X. Zhang, X. Wang, H. Chen, J. Zhao, L. Jiang, *Chem. Asian J.* **2014**, *9*, 1943.

[16] a) C. Lee, Y. Lai, S. Cheng, Y. Cheng, *Org. Lett.* **2014**, *16*, 936; b) Y. Fukutomi, M. Nakano, J. Hu, I. Osaka, K. Takimiya, *J. Am. Chem. Soc.* **2013**, *135*, 11445; c) CCDC 1034509 (**PyPT**) and 1063524 (**PyPS**) contain the supplementary crystallographic data for this paper. These data are provided free of charge by The Cambridge Crystallographic Data Centre.

[17] a) D. Fichou, *J. Mater. Chem.* **2000**, *10*, 571; b) L. Zhang, N. S. Colella, B. P. Cherniawski, S. C. B. Mannsfeld, A. L. Briseno, *ACS Appl. Mater. Interfaces* **2014**, *6*, 5327.

[18] H. Huang, Q. Fu, B. Pan, S. Zhuang, L. Wang, J. Chen, D. Ma, C. Yang, *Org. Lett.* **2012**, *14*, 4786.

[19] a) X. Wang, X. Zhang, Y. Wu, X. Ai, J. Zhang, Y. Wang, M. Sun, *Chem. Phys. Lett.* **2007**, *436*, 280; b) N. Kulisic, S. More, A. Mateo-Alonso, *Chem. Commun.* **2011**, *47*, 514.

[20] a) J. Xiao, X. Xiao, Y. Zhao, B. Wu, Z. Liu, X. Zhang, S. Wang, X. Zhao, L. Liu, L. Jiang, *Nanoscale* **2013**, *5*, 5420; b) Y. Li, T. Liu, H. Liu, M. Tian, Y. Li, *Acc. Chem. Res.* **2010**, *43*, 1496; c) H. Liu, J. Xu, Y. Li, Y. Li, *Acc. Chem. Res.* **2010**, *43*, 1496.

[21] Gaussian 09, M. J. Frisch, G. W. Trucks, H. B. Schlegel, G. E. Scuseria, M. A. Robb, J. R. Cheeseman, G. Scalmani, V. Barone, B. Mennucci, G. A. Petersson, H. Nakatsuji, M. Caricato, X. Li, H. P. Hratchian, A. F. Izmaylov, J. Bloino, G. Zheng, J. L. Sonnenberg, M. Hada, M. Ehara, K. Toyota, R. Fukuda, J. Hasegawa, M. Ishida, T. Nakajima, Y. Honda, O. Kitao, H. Nakai, T. Vreven, J. A. Montgomery, J. E. Peralta, Jr., F. Ogliaro, M. Bearpark, J. J. Heyd, E. Brothers, K. N. Kudin, V. N. Staroverov, R. Kobayashi, J. Normand, K. Raghavachari, A. Rendell, J. C. Burant, S. S. Iyengar, J. Tomasi, M. Cossi, N. Rega, J. M. Millam, M. Klene, J. E. Knox, J. B. Cross, V. Bakken, C. Adamo, J. Jaramillo, R. Gomperts, R. E. Stratmann, O. Yazyev, A. J. Austin, R. Cammi, C. Pomelli, J. W. Ochterski, R. L. Martin, K. Morokuma, V. G. Zakrzewski, G. A. Voth, P. Salvador, J. J. Dannenberg, S. Dapprich, A. D. Daniels, O. Farkas, J. B. Foresman, J. V. Ortiz, J. Cioslowski, D. J. Fox, Gaussian, Inc., Wallingford CT, **2009**.

Manuscript received: July 14, 2015
Accepted Article published: August 18, 2015
Final Article published: ■■ ■■, 0000

FULL PAPER

Twist and Shout: Two asymmetrical twistacenes **PyPT** and **PyPS** have been synthesized. Single crystal X-ray analyses showed that **PyPT** and **PyPS** have twisted structures with torsion angles of 26.65° and 26.59°, respectively. Their preliminary optoelectronic properties and self-assembly behavior were also investigated.

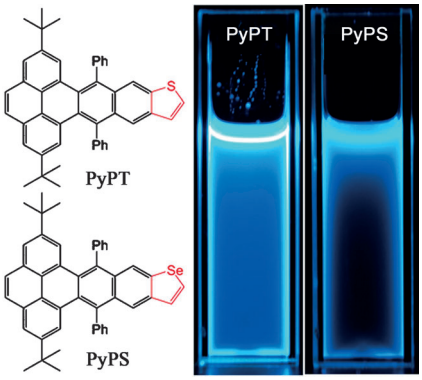

Fluorescence

Bo Lv, Xingxing Shen, Jinchong Xiao, Jingdan Duan, Xuefei Wang, Yuanping Yi**

■■ – ■■

Synthesis, Single Crystal, and Physical Properties of Asymmetrical Thiophene/Selenophene-Fused Twistacenes